

On the Modeling of Brine Transport in Porous Media

S. MAJID HASSANIZADEH AND TOON LEIJNSE

National Institute of Public Health and Environmental Hygiene (RIVM), Bilthoven, The Netherlands

The problem of concentrated brine transport arises in the study of transport of pollutants released from a repository in a rock salt formation. An important characteristic of brine, as compared to other solutions normally encountered in groundwater problems, is that it contains a high concentration of solutes. This factor requires special attention in the development of mathematical models for brine transport problems. In this work we discuss certain important physical and mathematical differences between low- and high-concentration situations. In particular, we consider three primary aspects of a model: basic equations, boundary conditions, and numerical techniques. Recognizing the fact that in high-concentration situations, the fluid motion is not independent of the solutes movement, a new formulation of Darcy's and Fick's law are proposed. The basic equations comprise a set of two nonlinear coupled partial differential equations to be solved for the pressure p and the solute mass fraction ω . These equations have to be solved by means of iterative methods. Various possibilities involving finite difference methods have been studied. In one case, after discretizing the equations in a fully implicit way, the Newton-Raphson method has been employed to solve the system of nonlinear difference equations simultaneously. In another case, after removing part of the nonlinearity by a transformation of the dependent variable ω , a procedure of sequential solution of the two equations by successive substitution is employed. It turns out that the latter method is considerably faster than the former one as a result of the quasi-linearization. Finally, considering boundary conditions, it is shown that often they are also nonlinear and coupled. Appropriate conditions for a rock salt boundary and an outflow boundary are developed and their significance in high-concentration situations are discussed. In particular, a nonlinear time-dependent boundary condition at a rock salt boundary is developed which takes into account the process of salt dissolution and cap rock formation.

INTRODUCTION

In recent years the problem of final disposal of hazardous waste (and in particular high-level radioactive waste) in salt formations has received increasing attention. In the event of escape of contaminants from such a repository, the most probable mechanism for release of pollutants to the biosphere is the transport of species via groundwater [cf. *International Atomic Energy Agency*, 1981]. It is known that in the vicinity of a salt dome or in aquifers which are in contact with bedded salt formations, brine densities higher than 1200 kg/m^3 exist [cf. *Siheeman*, 1963; *Visser*, 1974; *Sander and Herbert*, 1985]. High salt concentrations are not limited only to the proximity of salt domes. Also, in aquifers overlying salt formations the salt content varies from that of fresh water to that of saturated brine [cf. *Giesel and Fielitz*, 1983; *Boehme et al.*, 1985]. Also, brine and very saline water may be found in some crystalline rocks. Brine with density of 1204 kg/m^3 is encountered at a depth of 1500 m in the crystalline rocks of the Canadian Shield formation [*Frape et al.*, 1984]. High salt concentrations are also encountered in extensive aquifers in The Netherlands with a potential for the exploitation of geothermal energy [*Glasbergen*, 1981; *DGV-TNO*, 1983; *Mot*, 1984]. In these cases, salt concentrations as high as 1150 kg/m^3 have been observed. It must be noted that in such natural systems, the existence of high salt concentration gives rise to large concentration gradients as well. Therefore throughout this work it is assumed that in high-concentration situations, large concentration gradients also prevail.

There exist numerous models for the study of groundwater flow and solute transport problems, but they are mostly developed for situations where the solute concentration is equal to

or less than seawater concentration. These models employ assumptions and approximations which are not admissible at high concentrations. Recent theoretical studies indicate that for high-concentration situations one might need to modify the basic equations of flow and transport [*Hassanizadeh*, 1986b]. Also, recent studies have shown that some numerical schemes which work satisfactorily at low concentrations, need to be modified for high-concentration situations [*Leijnse*, 1985; *Herbert and Jackson*, 1986].

The purpose of this work is to illustrate and stress the need for more careful examination of ideas, equations, and methodologies employed for modeling of high-concentration transport problems. We consider three important aspects of a mathematical model: basic equations, boundary conditions, and numerical techniques. In the next section, based on the works of *Hassanizadeh* [1986a, b], a modified formulation of basic equations is presented and the effect of proposed modifications is illustrated by means of numerical experiments. In the third section, we discuss some possible boundary conditions which are applicable in high-concentration situations. Certain boundary conditions which are not admissible in these situations are indicated. Finally, a number of numerical schemes involving sequential solving and/or simultaneous iterative solution of nonlinear equations are discussed and their advantages and disadvantages are illustrated.

ON THE BASIC EQUATIONS

In the modeling of transport of N species by groundwater flow, generally, $N + 1$ sets of equations are employed: one set for each species and a final set for the flowing fluid. The set of equations for species constitutes the balance of mass of the species and a reduced equation of motion in the form of Fick's first law. Similarly, the set of equations for the flowing fluid constitutes the balance of mass of the whole fluid (consisting of the host liquid and species) and a reduced equation of

Copyright 1988 by the American Geophysical Union.

Paper number 7W4869.
0043-1397/88/007W-4869\$05.00

motion in the form of Darcy's law. If temperature changes are also of interest, an appropriate form of the energy equation should be added to the set of equations for the fluid. Also, if deformation of the porous medium and porosity changes are important, an additional set of equations for the solid phase of the porous medium has to be provided. In this study, however, we do not consider temperature or deformation effects.

In present practices of modeling of transport of low-concentration species in porous media, at least one of the following two restrictions are imposed: (1) all material properties such as mass density and viscosity of the flowing fluid and the dispersion coefficient are independent of species concentrations and/or (2) motion of the flowing fluid is independent of the motion of individual species. In any case, regardless of concentration values, normally the following formulation of Darcy's law and Fick's law are employed [Bear, 1979]:

$$\mathbf{q} = -\frac{\mathbf{k}}{\mu} \cdot (\nabla p - \rho \mathbf{g}) \quad (1)$$

$$\mathbf{J} = -\mathbf{D} \cdot \nabla \rho^s \quad (2)$$

where \mathbf{q} is the mean velocity of brine relative to the rock matrix, \mathbf{k} is permeability tensor, ρ and μ are mass density and dynamic viscosity of brine, p is the pressure, \mathbf{g} is the gravity vector, \mathbf{J} is the dispersive mass flux of salt, \mathbf{D} is the dispersion tensor, and ρ^s is the salt concentration. Note that although the term "Fick's law" commonly applies to molecular diffusion, we employ it in a wider sense to apply to (2) where \mathbf{D} is a function of velocity.

The assumptions mentioned above simplify the problem drastically. So that often one is able to solve the set of flow equations first and obtain fields of density, pressure, and velocity and then substitute these results in the set of equations for species which are solved subsequently to obtain species mass concentrations. Both of these assumptions, however, have to be reconsidered in high-concentration situations. Obviously, when the concentration of one or more of the species is high, the mass density and viscosity of the flowing fluid will be influenced by changes in concentration of these species. The main question, however, concerns the validity of Darcy's law and Fick's law at high salt concentrations. Darcy's law is shown, both experimentally and theoretically, to describe satisfactorily the flow of a single-phase low-concentration fluid under isothermal conditions. However, the authors have been unable to find in the literature experimental evidence of the applicability of Darcy's law and/or Fick's law to situations where high salt concentrations (and large concentration gradients) exist. On the contrary, recent theoretical studies have shown that both relations need to be modified for high-concentration situations. Hassanizadeh [1986b] has derived Darcy's and Fick's laws for a multicomponent fluid from fundamental principles of continuum mechanics. Following a rigorous thermodynamic approach, he has demonstrated that equations of motion of the fluid as a whole and its high-concentration components should contain cross-coupling terms. The general form of Darcy's law and Fick's law suggested by Hassanizadeh [1986b] for a two-component fluid are

$$\mathbf{q} = -\frac{\mathbf{k}}{\mu} \cdot (\nabla p - \rho \mathbf{g}^f) - \mathbf{D}^f \cdot \nabla \omega - \mathbf{M}^f \cdot (\mathbf{g}^s - \mathbf{g}^w) - \mathbf{T}^f \cdot \nabla T \quad (3)$$

$$\mathbf{J} = -\rho \mathbf{D} \cdot \nabla \omega - \omega \mathbf{K}^s \cdot (\nabla p - \rho \mathbf{g}^f) - \mathbf{M}^s \cdot (\mathbf{g}^s - \mathbf{g}^w) - \mathbf{T}^s \cdot \nabla T \quad (4)$$

where ω is the salt mass fraction; \mathbf{g}^s is the external body force (such as gravity and forces of electromagnetic fields) on the brine (superscript f) or its components (superscripts s and w); and T is the temperature. Note that in equations given by Hassanizadeh [1986b] there is also a $\nabla \rho$ term. However, because this can be converted to terms containing ∇p , $\nabla \omega$, and ∇T , we do not include it here.

Equations (3) and (4) contain all possible cross-coupling effects. Analogous equations to these have also been proposed by other authors in different fields. An equation similar to (4) has been suggested by Bird *et al.* [1960] for solute transport in fluids. In a recent article, Carnahan [1987] has suggested a similar set of equations to describe coupled processes in soils. Also, very closely related equations are employed to describe chemico-osmosis phenomena in fine-grained soils (see, for example, Michel [1976]). In the work of de Marsilly *et al.* [1987], if the chain rule of differentiation is employed to expand the term $\nabla \mu(p, \omega, T)$ (where μ is chemical potential), their equation for dispersive mass flux reduces to (4) above.

In the sequel, attention is confined to situations where temperature effects are negligible and no external body forces except gravity exist. Therefore to describe the flow of brine and transport of salt in porous media under isothermal conditions and assuming that the brine components do not react or adsorb, the following set of equations are employed.

Equations for the fluid

$$n \frac{\partial \rho}{\partial t} + \nabla \cdot (\rho \mathbf{q}) = 0 \quad (5)$$

$$\mathbf{q} = -\frac{\mathbf{k}}{\mu} \cdot (\nabla p - \rho \mathbf{g}) - \mathbf{D}^f \cdot \nabla \omega \quad (6)$$

Equations for salt

$$n \rho \frac{\partial \omega}{\partial t} + \rho \mathbf{q} \cdot \nabla \omega + \nabla \cdot \mathbf{J} = 0 \quad (7)$$

$$\mathbf{J} = -\rho \mathbf{D} \cdot \nabla \omega - \omega \mathbf{K}^s \cdot (\nabla p - \rho \mathbf{g}) \quad (8)$$

Equations of state

$$\rho = \rho_0 \exp(\gamma \omega + \beta(p - p_0)) \quad (9)$$

$$\mu = \mu_0(1 + m(\omega)) \quad (10)$$

where $m(0) = 0$. Parameters for (9) and (10) have been estimated using data from Weast [1982]. The following values are obtained at 20°C:

$$\rho_0 = 998.23 \text{ kg/m}^3 \quad \beta = 4.5 \times 10^{-10} \text{ m}^2/\text{N} \quad \gamma = 0.6923$$

$$m(\omega) = 1.85\omega - 4.10\omega^2 + 44.50\omega^3$$

The formulation for $m(\omega)$ is due to Lever and Jackson [1985], who have presented it in terms of a normalized mass fraction.

In this formulation, both restrictive assumptions mentioned earlier are avoided. First, ρ and μ are allowed to depend on the salt mass fraction ω , and the dispersive flux is formulated in terms of $\nabla \omega$. This is superior to the conventional formulation in terms of $\nabla \rho^s$ which is applicable only to situations where the fluid mass density is constant [Bird *et al.*, 1960, chapter 16]. Second, the motion of the fluid phase is coupled with that of the brine through inclusion of $\nabla \omega$ and $(\nabla p - \rho \mathbf{g})$

terms in (6) and (8), respectively. *Hassanizadeh* [1986b] has shown that these additional terms become negligible at low concentrations.

In order to investigate the effects of the additional terms suggested here, a number of numerical experiments have been carried out. The results are presented in Figures 1-5. Figures 1-3 give breakthrough curves for the salt components at the point $z = 0.25L$ along a vertical column of length L . In these calculations, first-type boundary conditions are employed at both ends of the column. Note that in all graphs given here, mass fraction values are normalized with respect to the mass fraction of the inflow.

In Figure 1, classical equations (i.e., $D^f = 0$ and $K^s = 0$) are solved for different salt mass fractions of the inflow fluid. It appears that when the salt concentration increases, the flow velocity decreases but at the same time the salt experiences more dispersion.

In Figures 2 and 3, the modified formulation is employed and breakthrough curves for various values of dimensionless numbers $\bar{D}^f = D^f \omega_0 \mu_0 / \rho_0 k$ and $\bar{K}^s = K^s \mu_0 / \rho_0 k$ are plotted. It is evident that depending on values assigned to these coefficients, very large differences in results may be obtained. Figures 4 and 5 give the peak value of (normalized) salt mass fraction at a given point in time and space plotted in terms of \bar{D}^f and \bar{K}^s , respectively. These figures illustrate that beyond certain critical values of these numbers the additional terms become important. From Figures 4 and 5 we obtain

$$\bar{D}_{crit}^f = 3 \times 10^{-4} \quad \bar{K}_{crit}^s = 2 \times 10^{-2} \quad (11)$$

Therefore if in an actual situation the measured values of \bar{D}^f and/or \bar{K}^s exceed these values, one must use modified Darcy's and Fick's equations. In order to illustrate the hydrological significance of these critical values for \bar{D}^f and \bar{K}^s , we have studied the results of experiments on chemical osmosis in clay

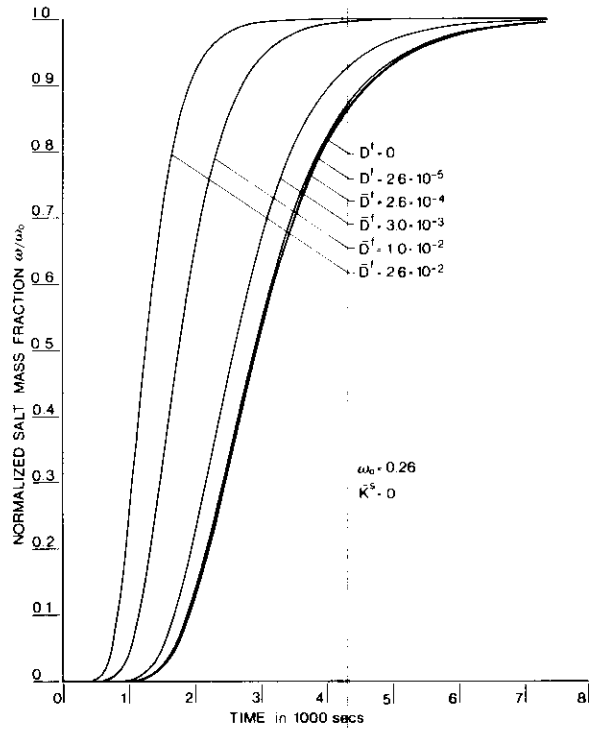


Fig. 2. Effect of coefficient D^f on breakthrough of salt at point $z = 0.25L$.

where equations similar to (6) and (8) are employed for describing the process. From definitions of \bar{D}^f and \bar{K}^s , it is evident that these numbers increase whenever the solute's mass fraction is high and/or the medium permeability is low. The latter situation is normally encountered in clay where chemo-osmotic effects are important. From results reported

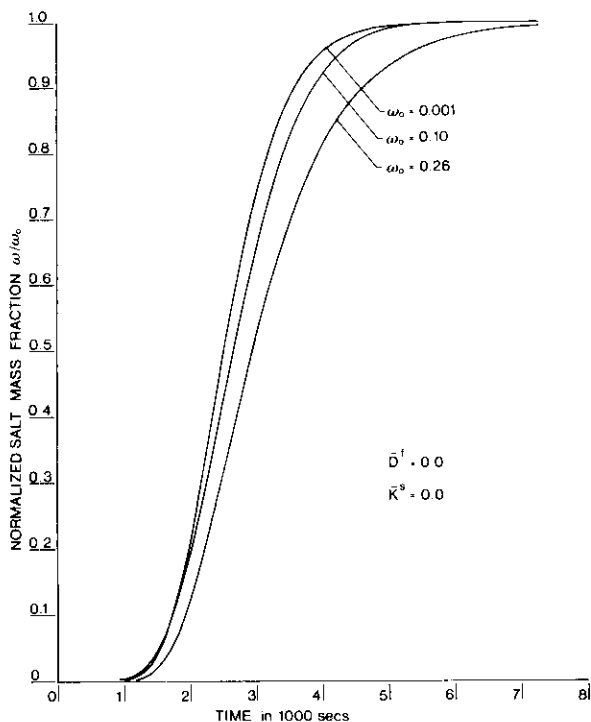


Fig. 1. Effect of maximum salt mass fraction on breakthrough of salt at point $z = 0.25L$.

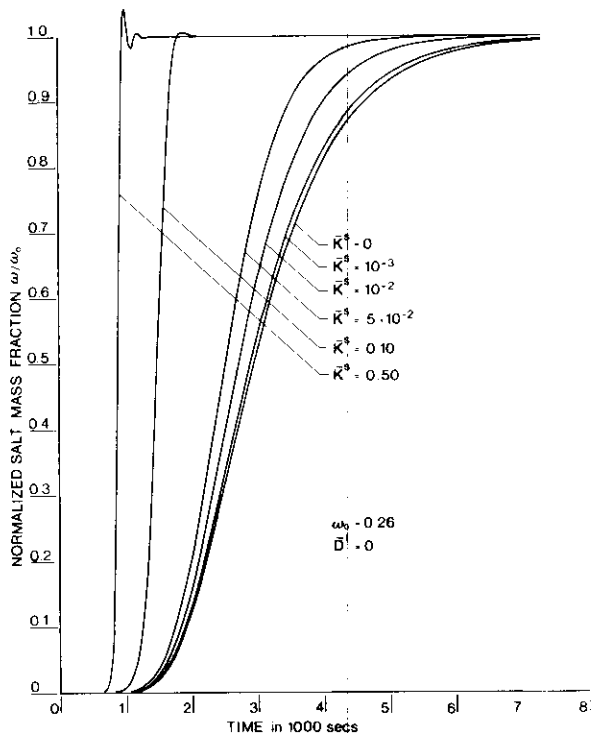


Fig. 3. Effect of coefficient K^s on breakthrough of salt at point $z = 0.25L$.

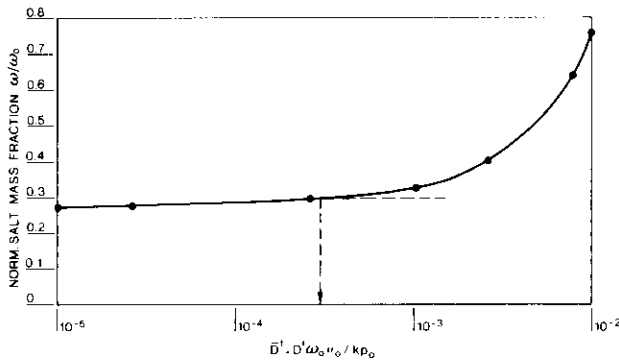


Fig. 4. Effect of coefficient D^f on the calculated value of salt mass fraction at point $z = 0.25L$ and at time $t = 2400$ s.

by Olsen [1972], \bar{D}^f was calculated for kaolinite to be 3×10^{-3} . Also based on results reported by Mitchel *et al.* [1973], \bar{D}^f and \bar{K}^s were calculated for bentonite to be 1.5×10^{-3} and 1.1, respectively. Obviously, these values are greater than the critical values given above and in fact chemico-osmotic effects have been quite noticeable in experiments of Olsen [1972] and Mitchel *et al.* [1973]. Laboratory experiments have to be conducted for evaluating the practical significance of these modifications in other soil types and for situations where high salt concentrations exist.

ON THE BOUNDARY CONDITIONS

One would expect the coupling which is inherent to the equations to affect the boundary conditions as well. In this section we demonstrate that this is in fact the case and often boundary conditions for flow and solute transport equations may not be chosen independently.

The key principle which must be observed in imposing boundary conditions is the continuity of total mass flux for any individual component as well as the net mass flux of the fluid across the boundary. Neglecting the velocity of rock matrix, the following relation for the net mass flux of brine at any given point may be written:

$$\rho \mathbf{q} = n \rho^w \mathbf{u}^w + n \rho^s \mathbf{v}^s \tag{12}$$

where ρ^w and ρ^s denote mass concentration of (pure) water and (pure) salt components of the brine ($\rho = \rho^w + \rho^s$) and \mathbf{v}^w and \mathbf{v}^s denote their respective velocities. From the definitions of the dispersive mass flux of salt \mathbf{J} and the salt mass fraction

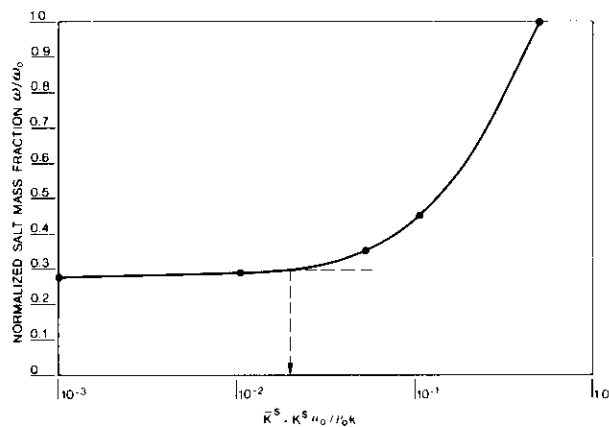


Fig. 5. Effect of coefficient K^s on the calculated value of salt mass fraction at point $z = 0.25L$ and at time $t = 2400$ s.

ω one has [Hassanizadeh, 1986b]

$$n \rho^s \mathbf{v}^s = \rho \omega \mathbf{q} + \mathbf{J} \tag{13}$$

such that (12) becomes

$$\rho(1 - \omega) \mathbf{q} = n \rho^w \mathbf{v}^w + \mathbf{J} \tag{14}$$

When the salt component is absent or exists at a very low concentration (such that $\omega \ll 1$ and $\mathbf{J} \ll n \rho^w \mathbf{v}^w$) one can write

$$\rho \mathbf{q} = n \rho^w \mathbf{v}^w \tag{15}$$

which emphasizes the fact that at low concentrations, the fluid motion is identified with the motion of (pure) water. Also, the latter relation illustrates why at low concentrations the flow and the transport boundary conditions may be specified independently.

To study the boundary conditions for high-concentration situations, two different physical boundaries are considered here: (1) an outflow boundary and (2) a rock salt boundary.

In what follows, each case is discussed separately. For the sake of simplicity, the boundaries are considered to be fixed. A numerical study of the boundary conditions here is not provided, because the one-dimensional models used in this work are not able to illustrate the differences between various formulations. Only a two- or three-dimensional model would be able to depict the actual effect of different boundary conditions.

An Outflow Boundary

This type of boundary is fairly well studied both for flow and transport problems. In general, one may assign a fixed pressure or a flux-type boundary condition for the flow. In any case, the continuity of the net mass flux for brine holds and one can write

$$\rho \mathbf{q}|_{b-} \cdot \mathbf{N} = \rho \mathbf{q}|_{b+} \cdot \mathbf{N} \tag{16}$$

where minus and plus signs designate the interior and exterior side of the boundary.

The most general boundary condition for the salt is the continuity of total salt mass flux across the boundary [Bear, 1979]:

$$(\rho \mathbf{q} \omega + \mathbf{J})|_{b-} \cdot \mathbf{N} = (\rho \mathbf{q} \omega + \mathbf{J})|_{b+} \cdot \mathbf{N} \tag{17}$$

In using this boundary condition, however, one has to model the outside reservoir as well. In that case, one needs an extra condition which is often obtained by assuming the continuity of concentration across the boundary. Modeling the exterior domain, however, is often not desirable. To avoid that situation, one may assume that the outside reservoir is well-mixed and the diffusion-dispersion phenomena there are negligible. Then, in the light of (16), we get

$$\mathbf{J}|_{b-} \cdot \mathbf{N} = 0 \tag{18}$$

This boundary condition commonly used in transport models [cf. van Genuchten and Parker, 1984] is not admissible in high-concentration situations because diffusive-dispersive mass fluxes at the boundary cannot be neglected. Therefore it can be used only far from the salt dome. In the domains of high concentration, however, (17) is the only feasible boundary condition for the salt transport equation.

If one is able to measure the salt mass fraction in the exterior reservoir as a function of time, a simple boundary condition would be to assume that

$$\omega|_{b-} = \omega^{\text{out}}(t) \tag{19}$$

This boundary condition, however, although can be used for laboratory experiments, is often not suitable for actual field situations. Often in a column experiment, ω^{out} can be measured and is known as a function of time. Then a more realistic boundary condition, which also allows for the discontinuity of concentration, would be

$$\rho q(\omega - \omega^{\text{out}})|_b = n^{\text{out}} \rho^{\text{out}} \frac{d\omega^{\text{out}}}{dt} (V/A)^{\text{out}} \quad (20)$$

where V is the volume of the outside reservoir and A is its cross-sectional area assumed to be equal to that of the column. This equation is obtained by combining integral equations of mass balance for the salt and for the whole fluid in the well-mixed outside reservoir.

A Rock Salt Boundary

Salt formations may appear in the form of a salt dome, a pillow salt, or a bedded salt formation [Harsveldt, 1980]. The physicochemical processes which take place at a rock salt boundary are quite difficult to model. However, because the time scale of thermodynamic changes at the boundary is much larger than that of the main flow domain, various degrees of simplification are possible. Note that boundary conditions discussed here are primarily considered for situations that as a result of certain phenomena, the present stable geohydrological conditions become disturbed. First, consider the case of a salt dome.

Geological investigations have shown that as the groundwater comes into contact with a salt dome and dissolves the salt away, a cap (residue) rock is formed at the salt dome surface; this is, of course, a very slow process. Based on geological studies in one specific site, a rate of growth of 0.04 mm/year for the cap rock thickness has been estimated [Bornemann and Fischbeck, 1986]. Although the cap rock has a low permeability, it is highly fractured and underneath it, the surface erosion of the salt dome proceeds. Thus the cap rock acts as a kind of resistance to the transfer of salt from the salt dome to the main flow domain. The salt concentration of brine at the salt dome side of the cap rock is equal to the saturation value at prevailing conditions [Boehme et al., 1985], and at the other side it is not known and is determined by the flow and transport processes in the main flow domain. Based on this picture, a boundary layer-type boundary condition is developed in Appendix B. Designating the cap rock thickness and its rate of growth by l and \dot{l} , respectively, and its porosity by n_c , we obtain the following boundary conditions.

For flow

$$\rho q|_b \cdot \mathbf{N} = [\rho_{ss}/a - \frac{1}{2}n_c(\rho_0^s + \rho|_b)]\dot{l} - \frac{1}{2}n_c l \frac{\partial}{\partial t} (\rho|_b) \quad (21)$$

For salt

$$(\rho \omega q + \mathbf{J})|_b \cdot \mathbf{N} = [\rho_{ss}/a - \frac{1}{2}n_c(\rho_0^s \omega_0^s + \rho \omega|_b)]\dot{l} - \frac{1}{2}n_c l \frac{\partial}{\partial t} (\rho \omega|_b) \quad (22)$$

Combining the two, we get

$$\mathbf{J}|_b \cdot \mathbf{N} = [(1 - \omega|_b)\rho_{ss}/a - \frac{1}{2}n_c \rho_0^s(\omega_0^s - \omega|_b)]\dot{l} - \frac{1}{2}n_c l \rho|_b \frac{\partial}{\partial t} (\omega|_b) \quad (23)$$

where $|_b$ indicates evaluation at the boundary of the main

domain, ρ_0^s is the mass density of saturated brine, and ω_0^s is its salt mass fraction, ρ_{ss} is the mass of salt per unit volume of the salt dome, a is the thickness of the layer of cap rock produced from a layer of the salt dome with unit thickness (see Appendix B). The ratio a is assumed to be known for a specific site.

As was mentioned earlier, one can specify typical values for l and, knowing its initial value, calculate \dot{l} at a given time. Then, (21) and (23), supplemented with Darcy's and Fick's equations and the equation of state, provide a set of boundary conditions for ω and p . These equations, however, are perhaps too general and rather difficult for practical applications. But they may serve as a basis for developing simpler boundary conditions and/or analyzing the boundary conditions commonly employed in mass transport problems; an example is given below.

Often, specific sites allow for certain simplifications of the general boundary conditions (21) and (23). For example, one feasible situation is where the brine contained in the cap rock remains always saturated. Therefore the saturation concentration is always situated at the entrance to the main domain. Thus for the transport equation, the following boundary conditions may be adopted:

$$\omega|_b = \omega_0^s \quad \text{and therefore} \quad \rho|_b = \rho_0^s \quad (24)$$

For the flow boundary condition, arguing that the rock salt is a solid boundary and thus "impermeable to flow," some researchers employ $\rho q|_b \cdot \mathbf{N} = 0$ [cf. Swedish Nuclear Inspectorate, 1986]. However, this boundary condition is not compatible with (24) because specifying the concentration implies (and in fact requires) a flow of salt across the boundary (thus $n \rho^s v^s$ is nonzero). Then, in the light of (12), $q \cdot \mathbf{N} = 0$ can not be admitted at rock salt boundaries. An appropriate boundary condition for the flow may be derived from (21) and (23). Substitution of (24) in these equations yields

$$\rho_0^s q|_b \cdot \mathbf{N} = \rho_{ss} \dot{l}/a - n_c \rho_0^s \dot{l} \quad (25)$$

$$\mathbf{J}|_b \cdot \mathbf{N} = (1 - \omega_0^s) \rho_{ss} \dot{l}/a \quad (26)$$

In (25), the first term on the right-hand side is the mass dissolved from the salt dome, and the second term is the mass of the brine formed within the new layer of cap rock; the difference between the two is the mass flux of brine which enters the main domain. Typically, the second term is two orders of magnitude smaller than the first and it can be neglected. Then, combination of (25) and (26) yields the following boundary condition for flow:

$$\rho_0^s (1 - \omega_0^s) q|_b \cdot \mathbf{N} = \mathbf{J}|_b \cdot \mathbf{N} \quad (27)$$

This equation simply states the continuity of total mass flux at the boundary provided that we assume the salt dome is impermeable to (pure) water. It can be directly obtained from (14) by setting $\omega = \omega_0^s$ and $\rho^w v^w \cdot \mathbf{N} = 0$ (because of the assumption that no water leaves or enters the salt dome). Note that after solving the problem with boundary conditions (24) and (27), (25) (or equally well (26)) can be used to estimate \dot{l} . We suggest (24) and (27) as feasible and compatible boundary conditions at a salt dome.

Equations (21)–(23) may be used to study the applicability of other commonly used inlet boundary conditions to a salt dome boundary. An example is the following boundary condition often used in low-concentration transport models [cf.

van Genuchten and Parker, 1984]:

$$(\rho(\omega - \omega_0^s)\mathbf{q} + \mathbf{J})|_b \cdot \mathbf{N} = 0 \quad (28)$$

This equation assumes that the inlet reservoir is well-mixed and the transition zone (the cap rock in our case) has a negligible storage. It can be shown that this boundary condition is not generally admissible in the case of a salt dome. Neglecting the storage terms in (21) and (22), multiplying the former with ω_0^s and subtracting from the latter equation one obtains

$$(\rho(\omega - \omega_0^s)\mathbf{q} + \mathbf{J})|_b \cdot \mathbf{N} = [(1 - \omega_0^s)\rho_{ss}/a + \frac{1}{2}n_c\rho(\omega_0^s - \omega)]l \quad (29)$$

The right-hand side is always positive and will be zero only if the dissolution of the rock salt may be neglected. This may be a good approximation for the presently stable geohydrological situations. But, in general, (27) together with condition (24) should be preferred.

At the boundary of a bedded salt or a pillow salt formation, where a well-defined cap rock does not exist, the salt concentration adjacent to the formation is equal to the saturation value. Also, in such cases, (24) and (27) may serve as feasible boundary conditions.

ON THE NUMERICAL SOLUTIONS

In principle, (5)–(10) supplemented with appropriate boundary and initial conditions must be solved simultaneously to obtain ρ , ω , p , μ , and \mathbf{q} . As is illustrated in Appendix A, by combining these equations, one obtains two equations for the unknowns p and ω . In general, it will not be possible to obtain closed-form analytical solutions and one has to resort to numerical techniques. Even then, strong nonlinearities of these equations will be challenging to any numerical scheme. In an attempt to obviate some of the nonlinearities, a transformation of the dependent variables ω and p is employed. Details of quasi-linearizations as well as nondimensionalization of equations are also given in Appendix A.

In this section, results of a series of one-dimensional simulations carried out for a vertical column containing a homogeneous porous medium are given. The governing equations, based on the classical forms of Darcy's law and Fick's law, were written in difference form by using either a backward difference scheme or a central difference scheme for the space derivative and a fully implicit formulation for the time derivative. The resulting nonlinear equations were solved either simultaneously by Newton-Raphson iteration, or sequentially by successive substitution. Basically, the following three schemes are considered: (1) using a backward difference scheme and sequential solution of (nonlinearized) (A3) and (A4) by successive substitution; (2) using a backward difference scheme and simultaneous solution of (nonlinearized) (A3) and (A4) by Newton-Raphson method; and (3) using a centered difference scheme and sequential solution of (quasi-linearized) (A8) and (A9) by successive substitution.

In this study the three following aspects of a numerical method are considered: (1) the efficiency of the method in terms of computer time, (2) differences between results obtained with different schemes, and (3) the convergence behavior of different schemes.

In all simulations the same values for physical parameters of the system were used. The dispersion coefficient was assumed to be linearly dependent on the velocity and molecular diffusion was neglected.

The initial condition for the salt mass fraction was $\omega = 0$ everywhere. Boundary conditions were specified pressure at both ends, $\omega = 0.26$ (saturated brine) at the bottom and $\omega = 0$ at the top. The boundary pressure values are such that an upward flow will develop, thus introducing salt into the system. As the amount of salt in the column increases, the velocity will decrease as a result of the increase in density and viscosity.

In the first series of simulations, the pressure difference across the system was high enough to maintain a flow upward at all times. In this case, the centered difference scheme (method 3) was not sensitive to the grid size when the number of grid blocks exceeded 40. Whereas the backward difference scheme (methods 1 and 2) still showed some changes in the results up to 160 grid blocks. As expected, increasing the number of grid blocks decreased the effect of numerical dispersion. With 160 grid blocks, the backward and the central finite difference schemes gave practically the same result, while for 80 grid blocks there were still some small differences.

Using 80 grid blocks, a comparison of the required CPU time for the three different schemes was made. To make the comparison meaningful, the same time step control (and hence the same number of time steps) was used and the same degree of accuracy in all simulations was required. Using the quasi-linearization and solving the difference equations sequentially by successive substitution (method 3) turned out to be the most efficient scheme. Solving the original equations sequentially with successive substitution (method 1) required on the average 20% more computer time. The simultaneous scheme, using Newton-Raphson method (method 2), required 160% more CPU time. Note that for these simulations, the time step was chosen small enough to ensure convergence for all schemes. Therefore it appeared that method 3 would converge faster than the other two methods.

In the second series of simulations, the pressure difference across the column was specified so that it was not enough to maintain an upward flow at all times. For such a boundary condition, the velocity will decrease until the transport of salt into the system stops altogether. This is because we have neglected molecular diffusion and at zero velocity, the dispersion coefficient will become zero.

Figures 6 and 7 show salt concentration profiles obtained with the backward and central finite difference schemes for 40 and 80 grid blocks. The profiles are given for very late times in the simulation when the velocities are very small. As one would expect, the curves for 80 grid blocks show smaller differences than the ones for 40 blocks. However, note that the differences for 80 grid blocks between the two methods are still much bigger than the ones which occurred in the "high pressure drop" situation.

Figure 8 shows the velocities that have been calculated using methods 2 and 3. The velocities for the backward finite difference scheme are in the order of 10^{-12} m/s, while the central difference scheme still shows velocities of 2×10^{-9} m/s. Although these differences are not significant, they may become important if one has to carry out simulations for a very long period of time, as is the case for the transport of radionuclides released from a repository in a rock salt formation. Further simulations are needed to find out how an increase in the number of grid blocks will change the velocity profiles and what the effect of molecular diffusion will be.

Also, the convergence behavior of different schemes has

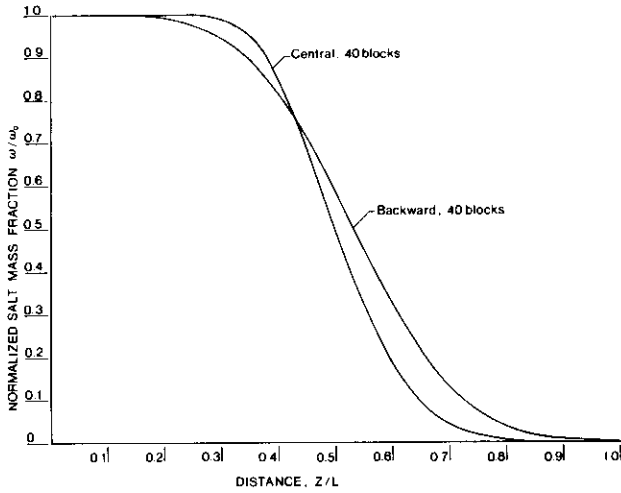


Fig. 6. Salt mass fraction profiles at time $t = 7080$ s calculated with the backward difference scheme and sequential solution of equations for the high pressure drop case.

been investigated. For both the high pressure drop and the "low pressure drop" systems, simulations have been carried out with increasingly relaxed restrictions on the time step control. For the ranges investigated, both methods broke down but only in the low pressure drop situations and at later times where the velocities become very small. Unexpectedly, the sequential methods performed even better than the Newton-Raphson method.

Finally, it must be noted that results presented in this section provide only some indications of the behavior of various numerical schemes at high-concentration situations. Because they are all based on one-dimensional simulations, they cannot be considered as completely conclusive. Two- and three-dimensional models will have to be employed to provide more definite results in this regard.

CONCLUSION

A new formulation of the equations describing brine flow and salt transport is provided. The equations are applicable to other mass transport problems involving high-concentration

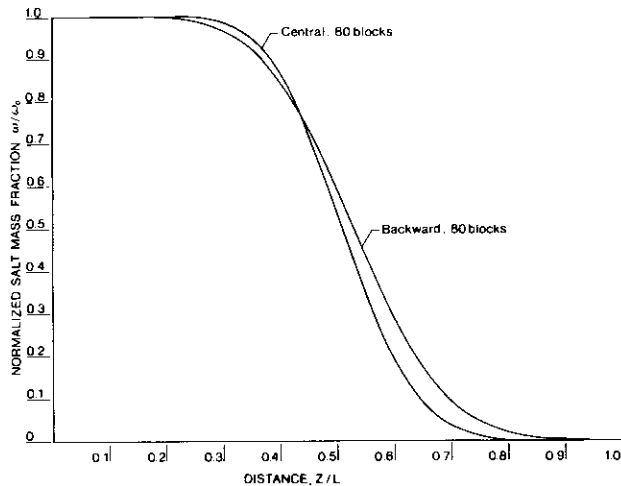


Fig. 7. Salt mass fraction profiles at time $t = 277,800$ s calculated with centered and backward difference schemes for the low pressure drop case.

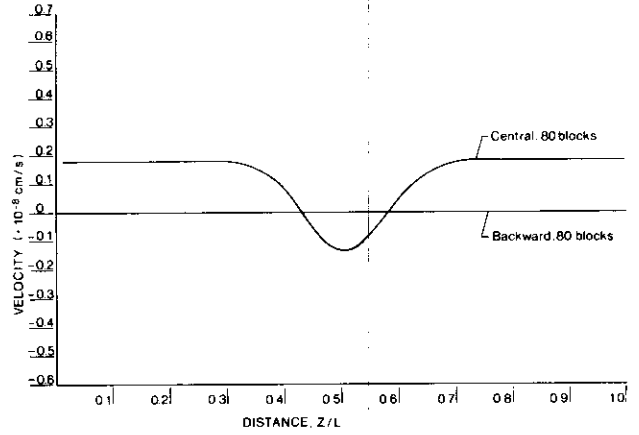


Fig. 8. Salt mass fraction profiles at time $t = 277,800$ s calculated with centered and backward difference schemes for the low pressure drop case.

solutes. In this formulation a modified version of Darcy's and Fick's laws derived by Hassanizadeh [1986b] are employed. These equations contain terms which account for the effect of high salt concentrations. By means of numerical experiments, the potential significance of proposed modifications in the basic equations are illustrated. It is found out that above certain critical values of the dimensionless numbers $\bar{D}^f = D^f \omega_0 \mu_0 / k p_0$ and $\bar{K}^s = K^s \mu_0 / \rho_0 k$ these modifications become important. This conclusion is supported by results from chemical osmosis experiments.

It is illustrated that at high concentrations, boundary conditions for flow and transport equations may not be chosen independently. Appropriate boundary conditions for an out-flow boundary and a rock salt boundary are developed. It is shown that certain boundary conditions while acceptable at low concentrations, are not admissible at high-concentration situations. For example, it is shown that a no-flow boundary condition ($\mathbf{q} \cdot \mathbf{N} = 0$) and a first-type boundary condition for salt ($\omega = \omega_0$) are not acceptable for a solid rock salt boundary. The set of boundary conditions given by (21) and (23) are the most general for a salt dome boundary, but simpler and yet feasible conditions are provided by (24) and (27).

Finally, advantages and disadvantages of certain numerical schemes in high-concentration situations are discussed. It is found out that sequential solution of quasi-linearized equations by successive substitution requires less CPU time and accepts bigger time steps.

APPENDIX A: NONDIMENSIONALIZATION AND QUASI-LINEARIZATION OF EQUATIONS

First, substitute ρ , \mathbf{q} and \mathbf{J} from (9), (6), and (8) into (5) and (7). The chain rule of differentiation should be employed to write derivatives of ρ in terms of those of ω and p . To nondimensionalize the equations, the following set of dimensionless variables and parameters are employed; the barred characters stand for dimensionless variables:

$$\begin{aligned}
 \bar{\rho} &= \rho / \rho_0 & \bar{\omega} &= \omega / \omega_0 & \bar{p} &= p / p_0 & \bar{\mathbf{D}}^f &= \mathbf{D}^f \omega_0 \mu_0 / p_0 k \\
 \bar{\mu} &= \mu / \mu_0 & \bar{\mathbf{q}} &= \mathbf{q} / q_r & \bar{t} &= t / t_r & \bar{\mathbf{D}} &= \mathbf{D} / q_r L \\
 \bar{\beta} &= \beta p_0 & \bar{\gamma} &= \gamma \omega_0 & \bar{\mathbf{k}} &= \mathbf{k} / k & \bar{\mathbf{K}}^s &= \mathbf{K}^s \mu_0 / \rho_0 k \\
 \bar{\nabla} &= L \nabla & \bar{\mathbf{g}} &= \rho_0 \mathbf{g} L / \rho_0 = G \mathbf{e}_g & G &= \rho_0 g L / \rho_0
 \end{aligned}
 \tag{A1}$$

where ω_0 is a reference value for the salt mass fraction, L is

the macroscopic characteristic length of the medium, k is a characteristic value for permeability of the medium, \mathbf{g} is the magnitude of gravity vector, and \mathbf{e}_g is its unit direction vector, and

$$q_r = k\rho_0/\mu_0L \quad t_r = L/q_r \quad (\text{A2})$$

The nondimensionalized equations read as follows. Note that in the interest of lucidity, the overbar notation is suppressed. However, all variables and parameters are understood to be dimensionless:

$$n \frac{\partial \omega}{\partial t} - \frac{1}{\rho} \nabla \cdot (\rho \mathbf{D} \cdot \nabla \omega) - \nabla \omega \cdot \bar{\mathbf{D}}^f \cdot \nabla \omega - \frac{\mathbf{k}}{\mu} \cdot (\nabla p - \rho G \mathbf{e}_g) \cdot \nabla \omega = \frac{1}{\rho} \nabla \cdot (\omega \bar{\mathbf{K}}^s \cdot (\nabla p - \rho G \mathbf{e}_g)) \quad (\text{A3})$$

$$n\beta \frac{\partial p}{\partial t} + n\gamma \frac{\partial \omega}{\partial t} - \frac{1}{\rho} \nabla \cdot \left(\frac{\rho}{\mu} \mathbf{k} \cdot \nabla p \right) - \frac{1}{\rho} \nabla \cdot (\rho \bar{\mathbf{D}}^f \cdot \nabla \omega) + 2\mathbf{k} \frac{G}{\mu} \cdot \mathbf{e}_g \cdot \nabla \rho + \rho \nabla \cdot \left(\frac{G}{\mu} \mathbf{k} \cdot \mathbf{e}_g \right) = 0 \quad (\text{A4})$$

$$\rho = \exp(\beta(p-1) + \gamma\omega) \quad (\text{A5})$$

It is apparent that the two important terms, $(1/\rho)\nabla \cdot (\rho \mathbf{D} \cdot \nabla \omega)$ and $(1/\rho)\nabla \cdot ((\rho/\mu)\mathbf{k} \cdot \nabla p)$ are strongly nonlinear in p and ω . In order to obviate part of such nonlinearities, the following transformations of dependent variables p and ω are employed:

$$\psi = e^{\gamma\omega} - 1 \quad (\text{A6})$$

$$\phi = e^{\beta(p-1)} - 1 \quad (\text{A7})$$

Note that at low concentrations and at low pressures we will have $\psi \rightarrow \gamma\omega$ and $\phi \rightarrow \beta(p-1)$. The quasi-linearized equations will read as follows. Note that in order not to make the equations too crowded, only the classical form of Darcy's and Fick's equations are used here and terms containing $\bar{\mathbf{D}}^f$ and $\bar{\mathbf{K}}^s$ have been neglected:

$$n \frac{\partial \psi}{\partial t} - \nabla \cdot (\mathbf{D} \cdot \nabla \psi) - \left(\left(\frac{\mathbf{k}}{\mu} - \beta \mathbf{D} \right) \cdot \nabla p - \rho G \frac{\mathbf{k}}{\mu} \cdot \mathbf{e}_g \right) \cdot \nabla \psi = 0 \quad (\text{A8})$$

$$n\beta \frac{\partial \phi}{\partial t} - \nabla \cdot \left(\frac{\mathbf{k}}{\mu} \cdot \nabla \phi \right) - (\nabla \omega - 2\beta\rho G \mathbf{e}_g) \cdot \frac{\mathbf{k}}{\mu} \cdot \nabla \phi + \left(n\beta\gamma \frac{\partial \omega}{\partial t} + \beta\rho G (2\nabla \omega \cdot \frac{\mathbf{k}}{\mu} \cdot \mathbf{e}_g + \nabla \cdot \left(\frac{\mathbf{k}}{\mu} \right) \cdot \mathbf{e}_g) \right) (\phi+1) = 0 \quad (\text{A9})$$

Although these equations look just as nonlinear as the set of equations (A3) and (A4), in practice, they proved to give less numerical problems. This is partly because most nonlinear terms here are multiplied by β which has a very small value and partly because the important terms $\nabla \cdot (\mathbf{D} \cdot \nabla \psi)$ and $\nabla \cdot (\mathbf{k}/\mu \cdot \nabla \phi)$ are now linearized. It should be pointed out that the transformations also affect boundary conditions favorably. That, however, depends on the specific boundary condition being considered.

APPENDIX B: DERIVATION OF A SALT DOME BOUNDARY CONDITION

We shall develop a boundary layer-type boundary condition whose main feature is to take into account the existence of the cap rock. It is shown that the cap rock is formed out of

the nonsoluble materials of the salt dome; this may amount to only 5–10% of the salt dome [Commission of European Communities, 1984]. When a layer of the dome is dissolved away, the residues, under the action of tectonic forces and overburden pressure, compress into a fractured rock. Therefore when a unit thickness of the salt dome is dissolved, the thickness of the cap rock grows only by a fraction a .

Assume that the flow and transport in the cap rock is one-dimensional and in the direction transverse to the extent of the cap rock and that the salt concentration within the cap rock varies linearly from ω_0^s at the salt dome side to ω at the main domain side. Denote the thickness of the cap rock at time t by l and assume that after a period of Δt , the cap rock thickness grows to $(l + \Delta l)$. This means that a layer of the salt dome with the thickness of $\Delta l/a$ has to be dissolved. Now, consider a control volume with the initial thickness of $l + \Delta l/a$ which evolves into $l + \Delta l$ after a period of Δt (see Figure B1). We can write the following equations of balance of total mass and balance of salt contained within the control volume.

For salt

$$\rho_{ss} \Delta l/a + n_c \frac{\rho\omega + \rho_0^s \omega_0^s}{2} \Big|_l = n_c \frac{\rho\omega + \rho_0^s \omega_0^s}{2} \Big|_{l+\Delta l} (l + \Delta l) + (\rho\mathbf{q}\omega + \mathbf{J})|_b \cdot \mathbf{N} \Delta t \quad (\text{B1})$$

For total mass

$$\rho_{ss} \Delta l/a + n_c \frac{\rho + \rho_0^s}{2} \Big|_l = n_c \frac{\rho + \rho_0^s}{2} \Big|_{l+\Delta t} (l + \Delta l) + \rho\mathbf{q}|_b \cdot \mathbf{N} \Delta t \quad (\text{B2})$$

In these equations, the first term is the total mass dissolved from the rock salt, the second term is the mass (of brine and salt in equations (B1) and (B2), respectively) present within the cap rock at time t , the third term is the total mass present within the cap rock at time $t + \Delta t$, and the fourth term is the flux of mass out of the cap rock and into the main domain. Rearrange (B1) and (B2), divide through by Δt , and take the limit as $\Delta t \rightarrow 0$ to obtain the following equations:

$$(\rho\mathbf{q}\omega + \mathbf{J})|_b \cdot \mathbf{N} = [\rho_{ss}/a - \frac{1}{2}n_c(\rho\omega + \rho_0^s \omega_0^s)]l - \frac{1}{2}n_c l \frac{\partial \rho\omega}{\partial t} \quad (\text{B3})$$

$$\rho\mathbf{q}|_b \cdot \mathbf{N} = [\rho_{ss}/a - \frac{1}{2}n_c(\rho + \rho_0^s)]l - \frac{1}{2}n_c l \frac{\partial \rho}{\partial t} \quad (\text{B4})$$

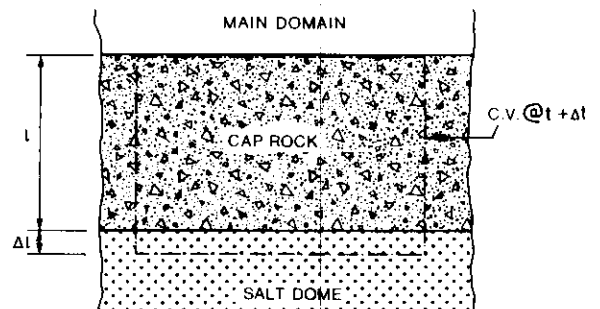


Fig. B1. Velocity profiles at time $t = 277,800$ s calculated with centered and backward difference schemes for the low pressure drop case.

NOTATION

- a thickness of the cap rock produced from dissolution of a layer of the salt dome with unit thickness (L/L).
- \mathbf{D} the dispersion tensor of salt (L^2/T).
- \mathbf{D}^f coefficient of density flow in the modified Darcy's equation, (L^2/T).
- \mathbf{g} gravity vector (L/T^2).
- \mathbf{g}^z external body force exerted on the brine and its components (L/T^2).
- \mathbf{J} diffusive-dispersive mass flux vector of the solute (M/L^2T).
- \mathbf{k} permeability tensor of the porous medium (L^2).
- \mathbf{K}^s pressure diffusion (–dispersion) coefficient in the modified Fick's equation (T).
- l thickness of the cap rock of the salt dome (T).
- L length of the column (L).
- \mathbf{M}^f (also \mathbf{M}^s) coefficients in the generalized Darcy's and Fick's equations (3) and (4).
- n porosity of the porous medium.
- n_c porosity of the cap rock.
- \mathbf{N} unit vector normal to a boundary.
- p thermodynamic pressure of the fluid (M/LT^2).
- p_0 reference pressure (M/LT^2).
- \mathbf{q} Darcy velocity (or specific discharge) vector of the fluid (L/T).
- t time (T).
- \mathbf{v}^s velocity of the salt component of the brine (L/T).
- \mathbf{v}^w velocity of the water component of the brine (L/T).
- z vertical coordinate along the column (positive upward) (L).
- β compressibility coefficient of brine (LT^2/M).
- γ coefficient of salt mass fraction in the brine density formula.
- ∇ the gradient (or divergence) operator ($1/L$).
- μ dynamic viscosity of the fluid (M/LT).
- μ_0 dynamic viscosity of water at reference conditions (M/LT).
- ρ fluid (intrinsic average) mass density (M/L^3).
- ρ_0 mass density of freshwater at reference conditions (M/L^3).
- ρ^s mass concentration of (pure) salt component of the brine (M/L^3).
- ρ^w mass concentration of (pure) water component of the brine (M/L^3).
- ρ_0^s mass density of saturated brine (M/L^3).
- ρ_{sv} mass of salt per unit volume of the salt dome (M/L^3).
- ω salt mass fraction ($=\rho^s/\rho)(M/M)$).
- ω_0^s salt mass fraction of saturated brine (M/M).
- l_b denotes evaluation at the boundary; plus indicates the exterior side and minus indicates the interior side of the boundary.

Acknowledgment. This work has been part of the research conducted under the contract F11W-0081-NL between the Commission of European Communities and the National Institute for Public Health and Environmental Hygiene (RIVM) of the Netherlands.

REFERENCES

- Bear, J., *Hydraulics of Groundwater*, McGraw-Hill, New York, 1979.
- Bird, R. B., W. E. Stewart, and E. N. Lightfoot, *Transport Phenomena*, John Wiley, New York, 1960.
- Boehme, J., et al., Grundwasserbewegung im deckgebirge uber dem salzstock Gorleben, datenermittlung, interpretation und modellrechnungen, *Rep. KWA 5107/3*, Fed. Inst. for Geosci. and Natl. Resour., Hannover, West Germany, 1985.
- Bornemann, O., and R. Fischbeck, Ablaugung und Hutgesteinsbildung am Salzstock Gorleben, *Z. Geol. Ges.*, 137, 71–83, 1986.
- Carnahan, C. L., Effects of coupled thermal, hydrological and chemical processes on nuclide transport, paper presented at Proceedings of Geoval Meeting, Swedish Nuclear Power Inspectorate, SKI, Stockholm, April 7–9, 1987.
- Commission of European Communities, PAGIS, Performance Assessment of Geological Isolation Systems, Summary report of phase 1, A common methodological approach based on European data and models, Comm. of European Commun., Luxemburg, 1984.
- De Marsilly, G., D. Fargue, and P. Goblet, How much do we know about coupled transport processes in the geosphere and their relevance to performance assessment?, paper presented at Proceedings of Geoval Meeting, Swedish Nuclear Power Inspectorate, SKI, Stockholm, April 7–9, 1987.
- DGV-TNO, Voorbereiding evaluatie boring aardwarmte, demonstratie project delfland, *Rep. 0853-29*, DGV-TNO, Delft, The Netherlands, 1983.
- Frape, S. K., P. Fritzs, and R. H. McNutt, Water-rock interaction and chemistry of groundwaters from the Canadian Shield, *Geochim. Cosmochim. Acta*, 48, 1617–1627, 1984.
- Giesel, W., and K. Fielitz, Evaluation of groundwater salinity from well logs and conclusions on flow of highly saline water, *Rep. 11656/83*, Fed. Inst. for Geosci. and Natl. Resour., Hannover, West Germany, 1983.
- Glasbergen, P., Extreme salt concentrations in deep aquifers in The Netherlands, *Sci. Total Environ.*, 21, 251–259, 1981.
- Harsveldt, H. M., Salt resources of The Netherlands as surveyed mainly by AKZO, in *Proceedings of the Fifth Int'l Symp. on Salt*, edited by A. H. Coogan and L. Kauber, pp. 65–81, The Northern Ohio Geological Society, Cleveland, 1980.
- Hassanizadeh, S. M., Derivation of basic equations of mass transport in porous media, 1, Macroscopic balance laws, *Adv. Water Resour.*, 9, 196–206, 1986a.
- Hassanizadeh, S. M., Derivation of basic equations of mass transport in porous media, 2, Generalized Darcy's and Fick's laws, *Adv. Water Resour.*, 9, 207–222, 1986b.
- Herbert, A. W., and C. P. Jackson, A study of salt transport in a porous medium: The application of NAMMU to HYDROCOIN level 1 case 5, *Rep. DoERW86121*, Harwell Lab., Oxfordshire, England, 1986.
- International Atomic Energy Agency, Safety assessment for the underground disposal of radioactive wastes, *Rep. 56*, Int. Energy Agency, Vienna, 1981.
- Leijnse, A., Modeling the flow of groundwater in the vicinity of a salt dome, in *Waste Management*, edited by R. G. Post, vol. 3, pp. 203–206, Ariz. Board of Regents, Tucson, 1985.
- Lever, D. A., and C. P. Jackson, On the equations for the flow of concentrated salt solution through a porous medium, *Rep. AERE R 11765*, Harwell, Lab., Oxfordshire, England, 1985.
- Mitchel, J. K., *Fundamentals of Soil Behavior*, John Wiley, New York, 1976.
- Mitchel, J. K., J. A. Greenberg, and P. A. Witherspoon, Chemo-osmotic effects in fine-grained soils, *J. Soil Mech. Found. Am. Soc. Civ. Eng.*, 99(SM4), 307–322, 1973.
- Mot, E., Nationaal onderzoekprogramma aardwarmte en warmteopslag, *Rep. NOA-1 1979–1984*, Projectbureau Energieonderzoek, Utrecht, The Netherlands, 1984.
- Olsen, H. W., Liquid movement through kaolinite under hydraulic, electric and osmotic gradients, *Am. Assoc. Pet. Geol. Bull.*, 56, 2022–2028, 1972.
- Sander, W., and H.-J. Herbert, NaCl crystallization at the $MgCl_2/NaCl$ solution boundary—A possible natural barrier to the transport of radionuclides, *Mineral. Mag.*, 49, 265–270, 1985.
- Stheeman, H. A., Petroleum development in The Netherlands, with special reference to the origin, subsurface migration and geological history of the country's oil and gas resources, *Verh. K. Ned. Geol. Mijnbouwkd. Genoot. Geol. Ser.*, 21, 57–95, 1963.
- Swedish Nuclear Inspectorate, HYDROCOIN, An international project for studying groundwater hydrology modeling strategies, Level 1 final report: Verification of groundwater flow models, Case 5, Swedish Nucl. Inspectorate, Stockholm, 1986.

- Van Genuchten, M.Th., and J. C. Parker, Boundary conditions for displacement experiments through short laboratory soil columns, *Soil Sci. Soc. Am. J.*, *48*, 703-708, 1984.
- Visser, W. A., Waste disposal and underground waters, *Geologie Mijnbouw*, *53*, 249-256, 1974.
- Weast, R. C., *Handbook of Chemistry and Physics*, 63rd ed., p. D261, CRC Press, Boca Raton, Fla., 1982.

S. M. Hassanizadeh and T. Leijnse, National Institute of Public Health and Environmental Hygiene (RIVM), P.O. Box 1, 3720 BA Bilthoven, The Netherlands.

(Received March 16, 1987;
revised November 16, 1987;
accepted November 17, 1987.)